

Received 25 November 2022, accepted 1 December 2022, date of publication 5 December 2022,
date of current version 8 December 2022.

Digital Object Identifier 10.1109/ACCESS.2022.3226688

RESEARCH ARTICLE

Advanced Coordination Method for Overcurrent Protection Relays Using New Hybrid and Dynamic Tripping Characteristics for Microgrid

FERAS ALASALI¹, ABDELAZIZ SALAH SAIDI^{2,3}, (Member, IEEE), NASER EL-NAILY⁴,
SAHBAN W. ALNASER⁵, (Member, IEEE), WILLIAM HOLDERBAUM⁶, (Member, IEEE),
SAAD M. SAAD⁴, AND MAHMOUD GAMAELDIN⁷

¹Department of Electrical Engineering, Faculty of Engineering, The Hashemite University, Zarqa 13133, Jordan

²Department of Electrical Engineering, College of Engineering, King Khalid University, Abha 61421, Saudi Arabia

³École Nationale d'Ingénieurs de Tunis, Laboratoire des Systèmes Électriques, Université de Tunis El Manar, Tunis 1068, Tunisia

⁴College of Electrical and Electronics Technology-Benghazi, Benghazi, Libya

⁵Electrical Engineering Department, Faculty of Engineering, The University of Jordan, Amman 11942, Jordan

⁶School of Science, Engineering & Environment, University of Salford, M5 4WT Salford, U.K.

⁷Power System Studies & Protection Unit, Saudi Aramco, Dhahran 34464, Saudi Arabia

Corresponding authors: William Holderbaum (w.holderbaum@salford.ac.uk) and Feras Alasali (ferasali@hu.edu.jo)

This work was supported in part by the Deanship of Scientific Research at King Khalid University through Research Groups Program under Grant RGP.2/81/43, and in part by the University of Salford and The Hashemite University (Renewable Energy Center).

ABSTRACT Nowadays, the Overcurrent (OC) and Earth Fault (EF) relays coordination problem is one of the most complex and challenging concerns of power protection and network operators due to the high and volatile generation capacity of renewable energy sources in the grid. In this article, a new and dynamic optimal coordination scheme based on a novel hybrid tripping characteristic has been designed and developed for Over Current Relays (OCRs). Considering the impact of renewable energy sources such as the photovoltaic (PV) system on fault characteristic, this work presents and verifies a novel dynamic and hybrid tripping to achieve minimum tripping time and improve the OCR and EF relays coordination performance in terms of security, sensitivity, and selectivity. The proposed dynamic and hybrid scheme will help the OCRs to cover the EF events, and it has been tested under different fault scenarios compared to the literature. The IEEE-9 and IEEE-33 bus systems are implemented in the ETAP package to validate the effectiveness of the proposed hybrid characteristics against traditionally well-established IEC characteristics. Furthermore, the performance of the proposed advance and dynamic protection approach which doesn't require a communication infrastructure is investigated for a power network with PV plants under different grid operation modes and topology to provide more robustness protection system. The results, as presented using Industrial software (ETAP), showed that the novel dynamic and hybrid tripping scheme improved the speed of the total time tripping different fault scenarios and location by more than 50% and covers all EF events compared to traditional OCR schemes from the literature. The proposed novel dynamic approach has superior performance in detecting high-impedance faults and significantly reducing the tripping time on the IEEE 33 bus network by 47%.

INDEX TERMS Over current relays, earth fault relay, dynamic coordination scheme, renewable energy sources, PV.

The associate editor coordinating the review of this manuscript and approving it for publication was Zhigang Liu¹.

I. INTRODUCTION

A. MOTIVATION AND LITERATURE REVIEW

The traditional power network system is a radial grid structure, therefore the grid operator today faces challenges in term of protection coordination due to Distributed Generations (DGs) such PV system. The impact of DGs on the distribution grid cannot be negligible where it causes serious problems in the planning, protection, and operation of the power grid [1], [2]. The capacity generation of DGs is yearly growing which affects the fault characteristics and contribution level at the power networks. In general, there are various types of faults in medium and low voltage network systems, where the Line-to-ground (LG) fault is considered as the most common fault and referred to as Earth-Faults (EF) [3], [4]. In power network equipped with DGs, the magnitude of LG fault current is low and volatile based on the DGs contributions, therefore there is a difficulty of recognizing this fault using traditional overcurrent or EF protection. LG fault normally increases phase voltage, which can lead to dielectric breakdown of grid equipment and cause a Line-to-Line faults [4]. Generally, Overcurrent Relays (OCRs) are commonly used as primary protection system at the distribution power grid. Traditional OCR protection characteristics (definite, inverse, instantaneous and mixed curves) are mainly focused on load and fault currents with their relation to tripping time [5]. However, traditional OCR characteristics do not consider the structural changes of the power network with DGs that impact load and fault characteristics. As discussed in [3] and [4], the LG fault occurs, and modern power network with DGs is difficult to identify and considered as complex challenge for grid operators.

Therefore, there is a need to develop different protection approaches and modify the traditional overcurrent criteria to improve the selectivity and sensitivity of the protection system. To overcome this problem, network operators need to add an EF protection system at all voltage levels in the network and coordination with existing OCR and directional OCR [4], [5], [6], [7]. However, this process is highly costs which can limit of having additional DGs in the grid. Based on these needs, this article proposes a fast and advanced coordination scheme for overcurrent protection relays using new dynamic and hybrid tripping characteristics. The proposed dynamic and hybrid tripping scheme aims to improve the functionality of the OCR in order to work as phase OCR and cover the EF relay by virtually adapting the fault and pick current component in the OCR based on the fault characteristics. In microgrid or distribution network system, designing and developing an optimal protection coordination scheme considering the impact of DGs for EF scenarios is complex task [4], [5]. This article proposes a dynamic and multifunctional scheme for the OCR which increase the reliability of the protection system and deal with these challenges and uncertainty in grounding systems. The proposed new hybrid and dynamic scheme will combine both functions of phase OCR and EF relays by virtually modifying the fault and pickup current inside the OCR.

Limited research is done on designing new OCR schemes for microgrid systems, including a power grid connected to DGs. In [7], an adaptive OCR protection approach is presented to deal with the issues of coordination of the earth and phase OC. El-Naily et al. [7] presented the OCRs coordination problem in IEC network system as an optimization problem and then solved it by using different optimization methods. Similarly, Polajžer et al. [4] used a self-adaptive DE method to achieve the optimal settings of ground-fault relays in microgrid system. Furthermore, Andruszkiewicz et al. [6] presented a multi-criteria scheme for solving the OCRs coordination problem with EF in medium voltage networks. However, the pervious literature [4], [5], [6], [7] developed optimal coordination or adaptive strategies based on using the traditional inverse time characteristic, which will limit the performance at low fault current. Table 1 provides a critical review and summarizes the main literature of OCR and EF relay protection strategies and schemes. Several researchers [1], [2], [3], [4], [5], [6], [7], [8], [9], [10] have not taken into account the earth relay, while [5] has not included the directional OCR. Furthermore, the authors in [11] investigated their proposed system using three phase fault (LLL) and line-to-ground (LG). The impact of DG and the type of the transformer connection have not considered for the different type of DG: Inverter-Based DG (IBDG) or Synchronous-Based DG (SBDG). Similarly, the approaches presented in the literature, as shown in Table 1, required communication between the relays, which will increase the cost and tripping time [12], [13], [14], [15], [16], [17], [18], [19], [20], [21], [22]. A limited number of research investigated the OCR and EF coordination problem together [4], [5], [6], [7], [8], [9], [10], [11], [12], [13], [14], [15], [16], [17], [18], [19], [20]. However, the authors in [4] did not consider the directional OCR and covered only low fault resistance. On the other hand, the authors in [20] tested his proposed protection method on traditional power network without taking into account the DG impact on the grid and the proposed approach by [20] require a communication link between the relays. In addition, both researches [4], [5], [6], [7], [8], [9], [10], [11], [12], [13], [14], [15], [16], [17], [18], [19], [20] used fixed protection approaches and did not show a high reliability during earth faults. To handle the protection coordination challenges in power network with DGs, an adaptive protective scheme is presented by [23]. The proposed adaptive protective scheme focused on the OCR coordination problem without considering EF. Aazami et al. [24] showed that conventional tripping characteristics can lead to a number of mis-coordination especially for directional OCR. In general, the recent literature focused on using new adaptive approaches to handle the OCR coordination problem in microgrid systems [23], [24], however, the proposed approaches did not take into account EF relays coordination or use them as part of their approaches. In 2020, Balyith et al. [25] introduced a non-communication-based time-current-voltage coordination approach for directional OCR in a microgrid system. However, the study in [25] did not include EF relays and only focused on dual-setting

TABLE 1. A critical review and summarizes the main literature on OCR and EF relay protection strategies.

	2012	2014	2016	2017	2017	2019	2020	2021	2022	2022	2022	2022	2022	Proposed approach
	[12]	[13]	[14]	[15]	[16]	[17]	[18]	[19]	[4]	[20]	[6]	[21]	[22]	
OC relay	✓	✓	✓	✓	✓	✓	✓	✓	✓	✓	✓	✓	✓	✓
Directional OC relay	✓	✓	✓	✓	✓	✓	✓	✓	✓	✓	✓	✓	✓	✓
Earth relay	x	x	x	x	x	x	x	x	✓	✓	x	x	x	✓
Type of fault	LLL LLG LG	LLL LLG LG	LLL LLG LLG LG	LLL LL LLG	LLL LL LLG LG	LLL LLG LG	LLL	LLL LG	LLL LLG LG	LLL LG	ALL	LLL LG	LLL LLG LG	LLL LLG LG
Fault resistance	0	0	0	0	0	0-30	0	0	0-5	0-100	0	NO	0-20	0-30
Transformer DG connection	x	x	x	x	x	x	✓	x	✓	x	x	x	x	✓
DGs	x	✓	✓	✓	✓	✓	✓	✓	✓	x	x	x	✓	✓
Type of DG	x	SGDG	SGDG	SGDG	SGD G	x	IBDG	SGDG	SGDG	x	x	x	SGDG	IBDG
Update phase relay device settings	x	x	x	x	x	✓	✓	x	✓	x	x	x	x	✓
High reliability in earth fault	x	x	x	x	x	✓	✓	x	✓	x	x	x	x	✓
Need for communication	x	x	x	x	x	✓	x	x	x	✓	x	x	x	x
voltage-restrained overcurrent relay	x	x	x	x	x	✓	✓	x	x	x	x	x	x	x
Modifying the fault and pickup currents (virtually)	x	x	x	x	x	x	x	x	x	x	x	x	x	✓

directional OCR. In this work, the proposed novel dynamic protection scheme will combine both the OCR phase and the EF relay functions to handle the protection challenges in microgrid systems, and it has been demonstrated and verified using two reference grids (IEEE 9 and 33 bus) equipped with PV systems to show the effectiveness of the proposed dynamic approach.

B. CONTRIBUTION, INNOVATIONS AND STRUCTURE OF THE PAPER

As discussed previously and shown in Table 1, there is limited research in considering the EF relay and OCR for a power network with DGs. In addition, to the authors’ knowledge, there is no research introducing a combined protection scheme for EF relays and OCR under different fault scenarios. In this article, a new hybrid tripping characteristics for EF relays and OCR to achieve minimum tripping time for a power network connected to DGs (two PV generation systems through four MVA transformers). The proposed coordination approach is considered as a cost-effective protection scheme without the need for an extensive communication infrastructure, and its performance is investigated under different fault scenarios. The key contributions of this article are described as follows:

- Designing a new optimization coordination task based on a novel hybrid tripping characteristics to present the OCR and EF relays coordination problem for a power network connected to IBDGs. The proposed new coordination task is designed by taking into account the relationship between the Zero, Z_0 , to positive, Z_1 , impedance ratio and faults. Nowadays with more DGs in the network, one of the most critical challenges for

network operators is achieving the proper setting of Z_0/Z_1 . Therefore, the new optimization task is developed and will be solved by using Particle Swarm Optimization (PSO) algorithm in order to achieve minimum total tripping time for relays under different fault scenarios and power protection constraints such as coordination time interval.

- Based on the proposed new hybrid and dynamic approach, the protection security, sensitivity, and selectivity are improved to be more assertive by virtually adapting the fault and pick current components in the OCR based on the fault characteristics, which allowing OCRs to cover the EF. In this work, the EF relay is assumed to be not available or not work during the fault scenarios. In addition, the performance of the proposed approach has been investigated under different faults characteristics and network topologies and compared to the literature (standard OCR protection schemes, as presented on Table 1).
- The literature in Table 1 and international standards, such as IEEE 1547-2018, assumed interconnection and grounding methods for interconnecting DGs without taking into account the different types of winding transformer configurations. As a result, many utilities have followed appropriate grounding strategies for each case individually [11]. For example, some utilities connect the DGs transformers via a (Delta-Y with ground) to provide a sufficiently low impedance grounding route. However, such methods may make ground protection governance unattainable due to the interconnection of several DGs. This article proposes an advanced and

dynamic protection method for a power network with PV plants under different fault scenarios and covers the challenges of connecting PV transformers to the grid. In addition, the proposed new hybrid approach does not require a communication infrastructure, which will help to reduce the cost and provide more robustness protection system. Therefore, the proposed protection scheme is tested with different impedance fault scenarios and different DG operation scenarios.

The rest of this article is structured as follows. Section 2 introduces the background theory for short circuits via grounding system in the microgrid (IEEE-9 BUS network). The problem statement for the OCR and EF relays protection coordination is presented in Section 3. Section 4 discusses the methodology of the new coordination approach for Microgrid system. The simulation results are presented and discussed in Section 5. Finally, the conclusions of this work are presented.

II. BACKGROUND THEORY

This section aims to describe the basic model and method between the protection scheme and short-circuit analysis. The DGs operation mode affects the characteristics of the fault currents, especially zero-sequence [1], [2], [3], [4], [5], [6], [7], [8], [9], [10], [11]. Firstly, the effect of grounding system on the zero sequence fault characteristics is discussed. Then, the characteristics of the ground fault with overvoltage are presented for a power network with IBDG.

A. EFFECT OF EARTHING SYSTEM ON ZERO SEQUENCE QUANTITIES

In the power system, there is a relationship and conflicting requirements with the grounding systems [11]. One of the critical elements to consider is the Zero, Z_0 , to positive, Z_1 , impedance ratio, known as the Z_0/Z_1 ratio, with reference to the fault location. The degree of grounding, Z_0/Z_1 ratio, mainly depends on the grounding arrangement, location, and structure [1], [2], [3], [4], [5], [6], [7], [8], [9], [10], [11]. The ratio of Z_0/Z_1 can be expressed as follows:

$$\frac{Z_0}{Z_1} = \frac{X_0}{X_1} - j \frac{R_0}{R_1} \tag{1}$$

where X_0 and R_0 are zero sequence of inductive and resistive, respectively. X_1 and R_1 are positive sequence of inductive and resistive, respectively. In general, the positive sequence impedance, Z_1 , of a power system is reactive, X_1 . From Equation (1), it's clear that the degree of grounding, Z_0/Z_1 , value is mainly depending on the type of power line (specification) which has specific characteristics. According to the IEEE Std. 142, the degree of grounding, Z_0/Z_1 , value has a direct impact on the fault characteristics (current and voltage) [3], [4], [5], [6], [7], [8], [9], [10]. In general, the degree of grounding, Z_0/Z_1 , directly impacts the voltage and the fault current's level at any location in the distribution system, as shown in Fig. 1 [4], [5], [6], [7], [8], [9], [10]. First, the three phase and double phase faults (LLL and LL) are constant with the different Z_0/Z_1 . However, the ground faults (LG and LLG)

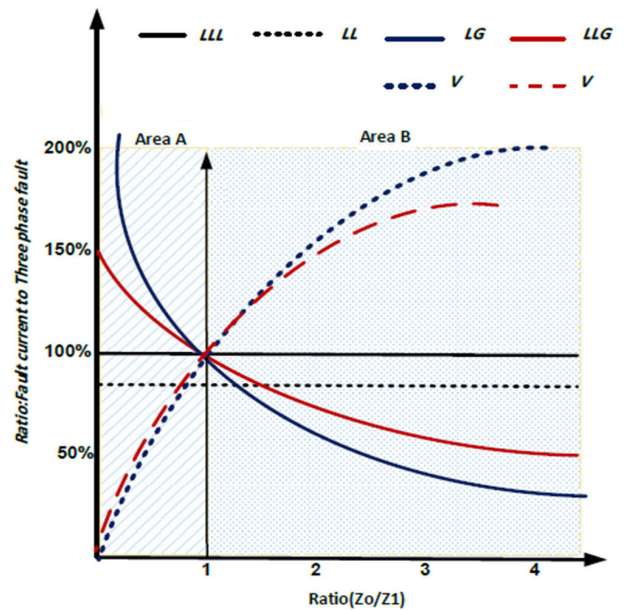


FIGURE 1. The relationship between the fault characteristics (current and voltage) and degree of grounding, Z_0/Z_1 , value.

which are the common fault are affected by Z_0/Z_1 . The LG and LLG faults are inversely proportional to Z_0/Z_1 which make it more volatile especially with DG. In area A, the $Z_0/Z_1 < 1$ and the LG and LLG faults are more than the LLL and LL faults. LG and LLG faults will be equal the LLL fault at $Z_0/Z_1 = 1$. The LG and LLG faults will be under the LLL and LL faults when $Z_0/Z_1 > 1$, as can see in area B in Fig. 1. This will let the ground faults be more challenging and difficult to detect. On the other hand, the voltage is directly proportional to Z_0/Z_1 ratio, where the over voltage can occur when the $Z_0/Z_1 > 1$. In this situation with the over voltages and small ground faults (area B), the power network will be at risk of equipment failure [3], [4], [5], [6], [7], [8], [9], [10], [11]. Today, with more DGs in the network, one of the most critical challenges for network operators is achieving the proper setting of Z_0/Z_1 . Therefore, it is required an advance protection scheme is required to handle these challenges, as presented in this article.

B. GROUND FAULT AND OVERVOLTAGE FOR A POWER NETWORK WITH IBDG

The increasing of capacity generation for DGs such as PV is in the power grid will lead to affect the Z_0/Z_1 value and then the level of ground fault and overvoltage. In general, when the transformers (directly grounded, Delta-Y) at PV plant interconnecting to the grid, the Z_0/Z_1 ratio in the network will substantially change and affect the ground faults. Accordingly, zero sequence current relays may not operate properly and lose their sensitivity to ground faults [11]. In case these transformers have been grounded at the high voltage side on the neutral point as a solution, the neutral voltage will be increased during LG and LLG faults. As result, when

the neutral voltage increases to a level higher than the gap breakdown voltage, the traditional protection system will trip and disconnect the PV transformers from the rest of the network. Disconnection and isolating many DGs from the network can cause serious stability problems [3], [4], [5], [6]. Therefore, the neutral voltage must be accurately estimated and considered to ensure that current gap protection does not operate inappropriately and cause network stability issues.

The international standards, for example IEEE 1547-2018, suggested interconnection and grounding methods for interconnecting transformers to the grid. However, these standards did not manage the different types of winding transformer configurations. For example, network operators connect the DGs transformers via a (Delta-Y with ground) to have low impedance grounding route. However, such methods increase the complexity of having a sensitive protection system and the protection governance will be unattainable due to the interconnection of several DGs with a low-impedance grounding route. This article proposes an advanced and dynamic protection method for a power network with PV plants under different fault scenarios and covers the challenges of connecting PV transformers to the grid.

III. THE PROBLEM OF COORDINATION OF OC/EF PROTECTION IN MICROGRIDS

The LG or LLG faults, as unbalance faults, are among the most common fault occur in the distribution system. Unlike balanced faults, ground faults rely on the grounding configuration (Z_0/Z_1 ratio), as shown in Fig.1. The fault level is mainly depending on the zero-sequence impedance and distribution transformer configurations. The variety in the nature of distributed sources with DGs creates operational challenges in events of ground faults. These challenges could influence the reliability of the OCR and EF protection system and make the coordination of different OCRs and EF relays in the complex microgrid unmanageable.

For example, the high share of multiple DGs in the grid during the fault event would cause a loss of coordination for the OCR protection scheme and unwanted operation of the fuse detection system. Fig. 2 shows the main fault characteristics based on the zones of the Z_0/Z_1 ratio (area A and area B), as presented in Fig1, and the miss-coordination between OCR and EF relay in the power network with DG. As previously discussed, the LG and LLG value will too small in area B, as shown in Fig.1 and Fig.2. The ground fault currents (LG and LLG) in area B can be seen by EF but will not be seen by OCR, which leads to miss-coordination, less reliability and delay in the total tripping time, as shown in Fig. 2. In case EF occurs at FD or FC, the current of LG and LLG faults will have a low value, and the EF relay represented by the green line will work without backup. Therefore, there is a need to operate OCR in area B as in A to avoid the miss-coordination events during ground fault events and minimize the disconnecting event for the DGs from the grid.

The power protection complexity in microgrids requires dynamic and multi-tasked protection schemes. This advanced

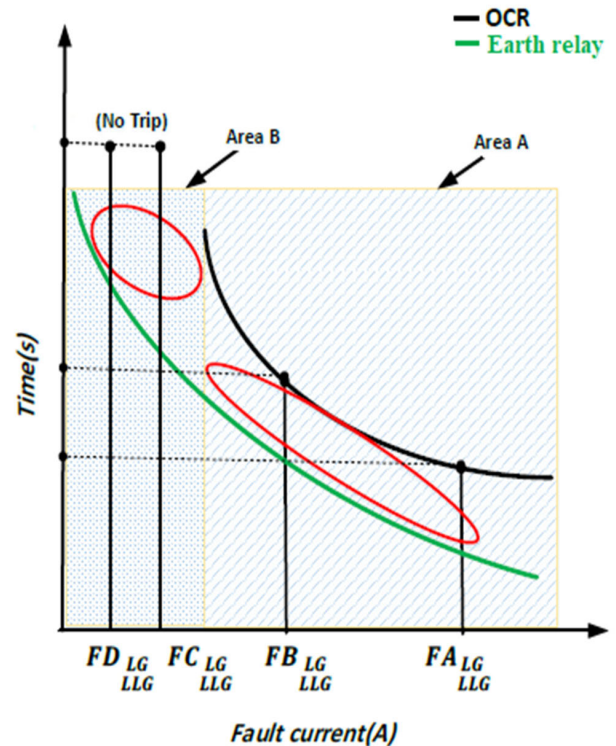


FIGURE 2. Characteristics of ground faults (LLG and LG) in the DG power network with DGs.

and dynamic scheme needs to provide protection for different fault scenarios and mainly ground faults (LG and LLG). This article proposes a dynamic and multifunctional scheme for the OCR which increase the reliability of the protection system and deal with these challenges and uncertainty in grounding systems. The new dynamic scheme will combine both functions of phase OCR and EF relays by virtually modifying the fault and pickup current inside the OCR.

IV. THE PROPOSED DYNAMIC HYBRID PROTECTION SCHEME

For all the challenges mentioned above, adapting the applicability and operation of OCR schemes to cover the EF protection schemes becomes urgently needed by modifying the functionality of OCR for both phase and ground fault events. In this study, a new dynamic characteristic is proposed to improve the functionality of the OCR scheme in ground fault situations by suggesting a modified hybrid current multiplier setting. The proposed modified hybrid scheme will adapt the function of the OCR to operate as a primary protection for high impedance faults when EF relays can't detect ground faults and as a local backup to reduce the overall operational time of the EF protection scheme. The significant development in nowadays-numerical relays fitted with well-practiced software provides practical solutions for the unique challenges in microgrids to improve the reliability and stability of the Microgrid against earth fault situations.

The traditional OCR operating time, t , is calculated based Equation (2) based on the fixed short-circuit current, I_{sc} , the pickup current, I_p , and the time multiplier setting, TMS. A and B are the relay parameters that determine the basis for the OCR relay standard, as discussed in [7], [8], [9], [10], [11], [12], [13], [14], [15], [16], [17], [18], [19], [20], [21], [22], [23], [24], [25], and [26].

$$t = \left[\frac{A}{\left(\frac{I_{sc}}{I_p} \right)^B - 1} \right] TMS \quad (2)$$

The proposed dynamic and hybrid OCR protection strategy aims to improve the functionality of the OCR to work as phase OCR and cover the EF relay. In order to cover all the OCR and EF relay functions, the proposed dynamic hybrid protection scheme has designed to include two sub-dynamic schemes, as follows:

- The first sub-dynamic scheme (area A) aims to avoid miss-coordination and cover all the earth faults and low fault current contributed in microgrid from PV which improve the reliability of the protection system by virtually increasing the fault current component.
- The second sub-dynamic scheme (area B) works on protecting and covering all possible phase and earth faults in the power grid with DGs and minimize the tripping time and improve the reliability of the protection system by adapting the pickup current.

Fig. 3 shows different ground fault currents (LG and LLG) to illustrate the practiced application of the proposed hybrid characteristics. For faults (FA and FB) in area A, the high

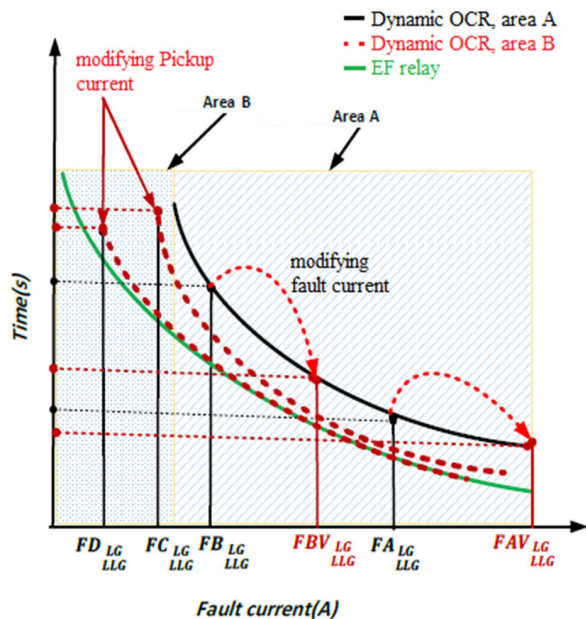


FIGURE 3. Characteristics of ground fault (LLG and LG) in the power network with DGs with the proposed dynamic and hybrid protection scheme.

level of earth faults (FA and FB) will initiate a trip signal in the EF relay (green curve) to work as a primary relay. The dynamic and hybrid current and multiplier settings for the OCR in this case (area A) will be virtually increasing the fault current component, represented by the black line in Fig. 3, which led to reducing the overall operational time for the OCR. As a result, this practice will enhance the reliability and speed in the event of high-level earth fault currents. The operating time for the OCR based on the proposed dynamic scheme for the faults in area A, t_{DA} , will be calculated based on Equation (3).

$$t_{DA} = \left[\frac{A}{\left(\frac{I_{sc} * k \left(\frac{i_0 - i_e}{I_p} \right)}{I_p} \right)^B - 1} \right] TMS \quad (3)$$

where k is constant equal to 5 that is optimally determined in this study to increase fault currents and then minimize the tripping time. i_0 and i_e are the zero-sequence current and earth relay current, respectively. For example, the fault current at point FB will be increase and modified to be located at point FBV, as shown in Fig.3 (red line). This modification helps to minimize the tripping time for all ground faults (LG and LLG) To the authors' knowledge, this process is not introduced in the literature.

The distinction and advantages of the proposed characteristic will be more evident for Faults (FC and FD) in area B, as shown in Fig.3, with the minimum ground fault current which will be the case during islanded mode and IBDG fault contribution. In this case, the traditional OCR will not be able to detect the EF, therefore, the proposed solution to modifying the pickup current in this area to let the OCR able to see the EF. In Fig. 3, faults FC and FD will be lower than the pickup current of the EF relay and will not be detected and cause the faults to remain and create stress on the equipment in the DN. The modifying of the fault current level as suggested for area A will not be applicable. Therefore, the proposed hybrid model is virtually reducing the pickup current in the OC relay and relocate the OCR characteristic to a new location to cover the area B, represented by dashed red line in Fig. 3.

The modification in the OCR scheme by adapting the pick current helps to minimize the tripping time for all ground faults (LG and LLG) and avoid the miss-coordination in area B. To the authors knowledge, this process does not introduce in the literature and the operating time for the OCR based on the proposed dynamic scheme for the faults in area B, t_{DB} , will be calculated based on Equation (4).

$$t_{DB} = \left[\frac{A}{\left(\frac{I_{sc}}{I_p * g \left(\frac{i_0 - i_e}{I_p} \right)} \right)^B - 1} \right] TMS \quad (4)$$

where g is a constant equal to 0.3 which optimally determined in this study by testing different values between 0.1 and 0.9 to reduce the pickup current to a value can help to achieve the minim tripping time. For example, the ground fault current at

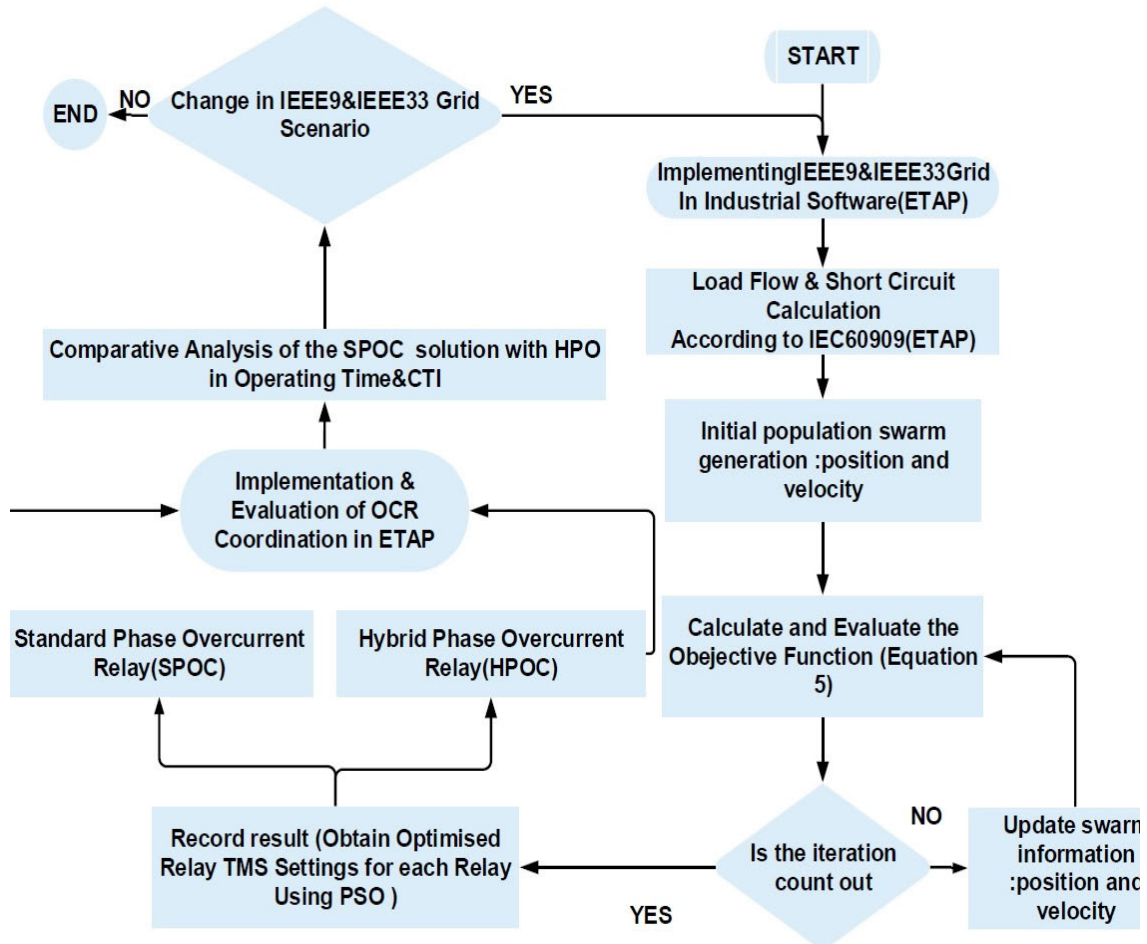


FIGURE 4. A flow chart of the proposed coordination scheme (HPOC).

point FD and FC was not cover by the OCR, the adaptive OCR scheme (dash red lines) help to avoid the miss-coordination issue in area B and minimize the total tripping time. and dynamic will be increase and modified to be located at point FBV, as shown in Fig.3 (red line).

The overall operational time of OCR, t , can be described as the summation of the time at two sub-dynamic schemes, as presented in Equation (5).

$$t = t_{DA} + t_{DB} \quad (5)$$

A. OCRS COORDINATION PROBLEM: FORMULATION AND OPTIMIZATION METHOD

The OCR coordination problem for a power network with DGs can be formulated as an objective function to the minimum operating time of OCRs and without miss-coordinate events. The following mathematical formulation is designed to enhance the OCR performance in areas A and B, as shown in Fig.3, using the proposed dynamic and hybrid protection scheme. The objective function for the OCR coordination problem is to be total tripping time, T , for the OCRs which need to minimized. The coordination problem is expressed in Equation (6) to minimize the tripping time of OCRs (t), for N

number of OCRs and Q number of fault locations.

$$T = \text{Min} \sum_{n=1}^N \sum_{q=1}^Q t_{n,q} \quad (6)$$

In a power network with N number of OCRs, the selectivity between primary and backup OCR relays can be obtained by formulating the constraint to manage and secure the time delay between each primary (t_{primary}) and backup (t_{backup}) OCR relays. The proper optimized Coordination Time Interval (CTI) constraint will ensure the selectivity among all OCR relays in the grid as follows:

$$t_{\text{backup}} - t_{\text{primary}} \geq \text{CTI} \quad (7)$$

The CTI is usually determined in the literature between 0.2 and 0.5 seconds according to IEEE-242 [8], [9], [10] and is been selected to be 0.3 seconds in this study. In addition, to ensure the sensitivity and selectivity of the protection system, the optimization problem in Equation (6) will be solved under the CTI constraint, as described in Equation (7), and the limitation of the operational time and TMS, as described in Equations (8) and (9).

$$t_{\text{min}} \leq t_n \leq t_{\text{max}} \quad (8)$$

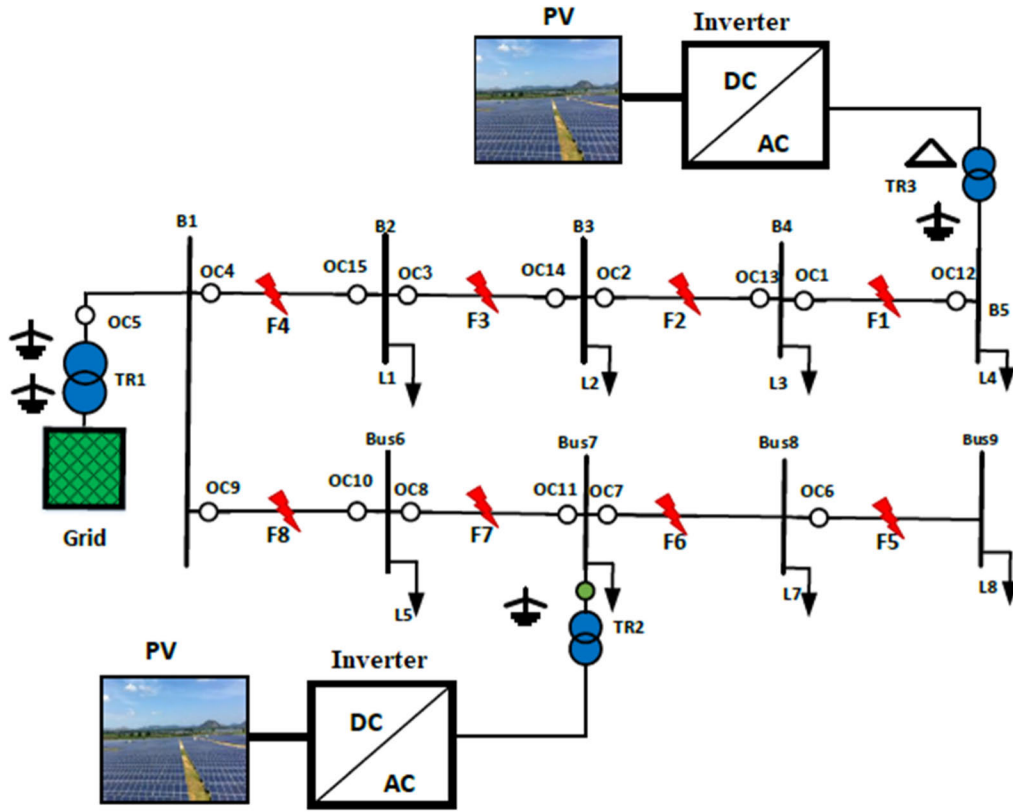


FIGURE 5. IEEE 9 bus Microgrid system.

TABLE 2. The OCR data in the proposed network model.

Relay	Type	CTR	IP	IPZ
OC1	non-directional	400/1	360	36
OC2	non-directional	400/1	360	36
OC3	non-directional	400/1	360	36
OC4	non-directional	400/1	360	36
OC5	non-directional	400/1	360	36
OC6	non-directional	400/1	360	36
OC7	non-directional	400/1	360	36
OC8	non-directional	400/1	360	36
OC9	non-directional	400/1	360	36
OC10	directional	400/1	280	36
OC11	directional	400/1	280	28
OC12	directional	400/1	280	28
OC13	directional	400/1	280	28
OC14	directional	400/1	280	28
OC15	directional	400/1	280	28

TABLE 3. The fault locations and impedance and admittance in the network.

Location of fault	Z_0/Z_1	
	Mode 1	Mode 2
F1	3.19	1.111
F2	2.936	1.216
F3	2.819	1.23
F4	2.651	1.242
F5	3.19	1.424
F6	2.936	1.136
F7	2.819	1.189
F8	2.651	1.192
B1	2.4	1.115
Feeder	6.01	3.7

$$TMS_{min} \leq TMS_n \leq TMS_{max} \quad (9)$$

where t_{min} and TMS_{min} are the minimum tripping time and TMS, respectively, t_{max} and TMS_{max} are the maximum tripping time and TMS, respectively, and t_n and TMS_n are the tripping time and TMS for relay n, respectively.

In this work, the TMS_{min} equal to 0.01 and TMS_{max} equal to 3 [7].

B. PARTICLE SWARM OPTIMIZATION

The Particle Swarm Optimization (PSO) algorithm is one of the common and efficient heuristic optimization methods for different applications. The PSO algorithm requires less memory and computational process to achieve an optimal solution

TABLE 4. The TMS for OCR in the power network.

Relay	Mode 1	Mode 2
	TMS	TMS
OC1	0.05	0.05
OC2	0.1611	0.162
OC3	0.2765	0.279
OC4	0.3970	0.403
OC5	0.5231	0.536
OC6	0.0500	0.05
OC7	0.1608	0.171
OC8	0.2728	0.293
OC9	0.3894	0.415
OC10		0.05
OC11		0.058
OC12		0.075
OC13		0.067
OC14		0.058
OC15		0.05

[26], [27]. The PSO algorithm introduced by Kennedy and Eberhart based on the general human sociality and swarming formulation of animal behavior. The PSO Technique aims to offer agents (called swarm), each of which provides potential solutions. Each agent preserves its present and optimum position towards the assigned objective function. The agents will locate a better position based on the particle movement. Finally, the PSO model will assign the optimum global solution among all possible solutions offered through each iteration [26], [27].

In this study, the PSO algorithm is employed to solve the OCRs coordination problem based on these advantages. Fig. 4 shows a flow chart of the PSO algorithm in solving the OCRs coordination problem. Firstly, the structure of the network (IEEE 9 BUS) is implemented by using ETAP simulation tool. To determine the initial OCR setting, the calculation of load flow and faults will be carried based on IEC 60909. These settings will be used as an initial solution population (particle) in the PSO algorithm. The process of the PSO to find the optimal setting is started by calculating and evaluating the solution population (particle). The particle trajectory and population will be updated based on the position of the best solution. The PSO process will be finished when the maximum number of iteration models has been achieved and the best solution will be use and apply to the proposed Hybrid Phase Overcurrent (HPOC) relay and compare the performance to the Standard Phase Overcurrent (SPOC) relay by using ETAP software under different fault scenarios and network operation mode.

V. SIMULATION RESULTS AND DISCUSSION

The power protection coordination problem, as presented in Section 3, and the proposed dynamic hybrid protection scheme, as discussed in Section 4, are evaluated using a standard distribution system. In this work, two benchmarks power grid equipped with PV plants are used to investigate the performance of the proposed dynamic hybrid protection

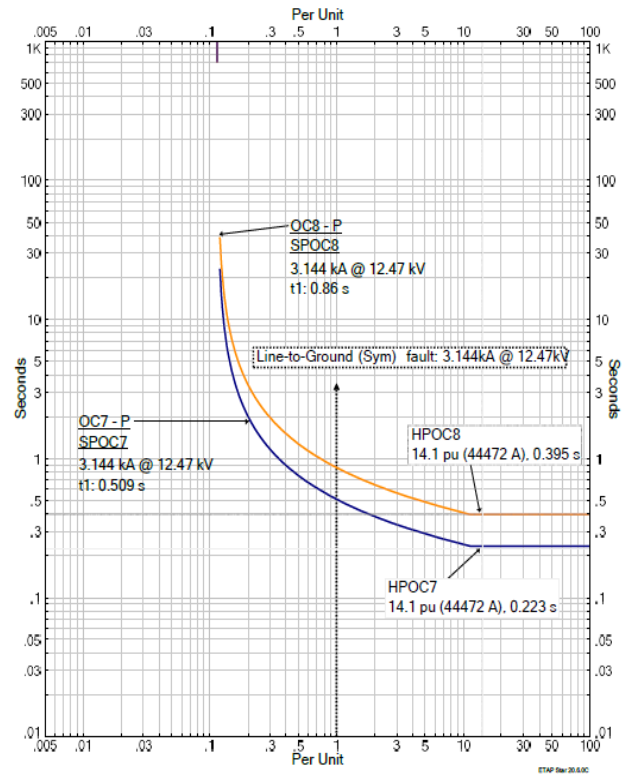


FIGURE 6. Time-current characteristics of OC7 and OC8 in Scenario 1 (R=0 ohm) for Mode 1 and LG fault.

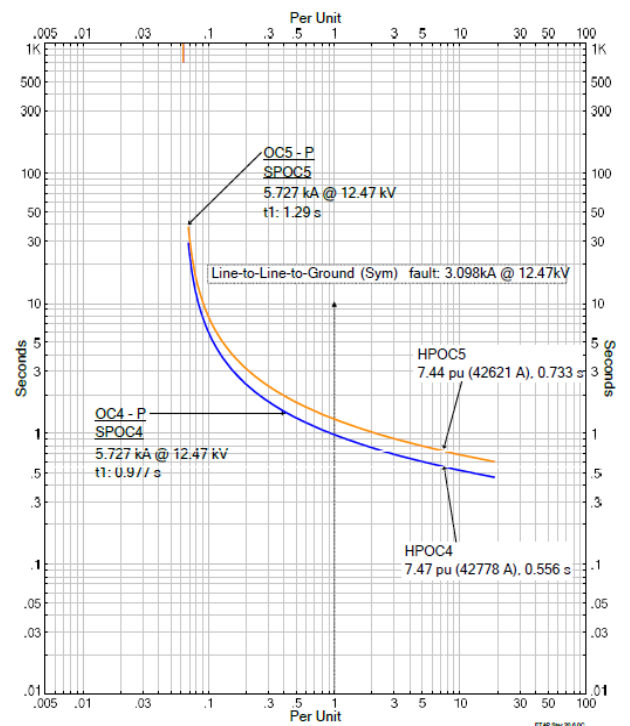


FIGURE 7. Time current characteristics of OC4 and OC5 at scenario 1 (R=0 ohm) for Mode 1 and LLG fault.

and compared to traditional schemes for different fault levels (minimum and maximum) as follows:

TABLE 5. The short-circuit analysis and TMS setting for OCR based on SPOC and HPOC approaches (Mode 1, Scenario 1).

Location of fault	Relays	LG	i_o	$\frac{i_o - i_e}{I_p}$	IFV	SPOC	HPOC	LLG	i_o	$\frac{i_o - i_e}{I_p}$	IFV	SPOC	HPOC
		R=0							R=0				
LG								LLG					
F1	OC1	2794	930	2.48	37125	0.167	0.074	2030	676.66	1.77	18063.24	0.19	0.085
	OC2	2794	930	2.48	37125	0.542	0.23	2030	676.66	1.77	18063.24	0.64	0.276
F2	OC2	3144	1048	2.81	44173	0.512	0.238	2300	766.66	2.02	23340.74	0.59	0.25
	OC3	3144	1048	2.81	44173	0.872	0.39	2300	766.66	2.02	23340.74	1.02	0.44
F3	OC3	3585	1195	3.21	57539	0.821	0.40	2646	882	2.35	31090.5	0.95	0.41
	OC4	3585	1195	3.21	57539	1.18	0.58	2646	882	2.35	31090.5	1.36	0.599
F4	OC4	4149	1383	3.74	77586	1.1	0.58	3098	1032.667	2.76	42884.35	1.26	0.55
	OC5	4149	1383	3.74	77586	1.46	0.75	3098	1032.667	2.76	42884.35	1.6	0.72
F5	OC6	2794	930	2.48	37125	0.167	0.074	2030	676.66	1.77	18063.24	0.19	0.085
	OC7	2794	930	2.48	37125	0.542	0.23	2030	676.66	1.77	18063.24	0.64	0.276
F6	OC7	3144	1048	2.81	44173	0.512	0.238	2300	766.66	2.02	23340.74	0.59	0.25
	OC8	3144	1048	2.81	44173	0.872	0.39	2300	766.66	2.02	23340.74	1.02	0.44
F7	OC8	3585	1195	3.21	57539	0.821	0.40	2646	882	2.35	31090.5	0.95	0.41
	OC9	3585	1195	3.21	57539	1.18	0.58	2646	882	2.35	31090.5	1.36	0.59
F8	OC9	4149	1383	3.74	77586	1.1	0.58	3098	1032.66	2.769	42884.35	1.2	0.55
	OC5	4149	1383	3.74	77586	1.46	0.75	3098	1032.66	2.76	42884.35	1.6	0.72

- IEEE 9-bus equipped with PV plants.
- IEEE 33-bus system, including plants (large scale of distribution network)

In addition, the dynamic hybrid protection scheme was tested under different network based on the availability of DGs in the network. First, the following section presents the description of the power distribution network under study. Then, the results of the standard and traditional OC scheme (SPOC) are presented to highlight the coordination problem. In this section, the dynamic hybrid protection scheme (HPOC) will be compared to the SPOC over different fault and network operation scenarios in terms of minimum total tripping time. The SPOC and HPOC approaches have been tested using Industrial software (ETAP), and results are presented. Throughout this section, the proposed and conventional schemes (HPOC and SPOC) will be evaluated and compared based on the network topology with and without DES (PV plants). Additionally, LG and LLG faults are generated within three different resistance fault scenarios. The fault resistances (R) are conceded to be equal to as 0, 10 and 30 Ohm to investigate the impact of the different fault scenarios on the proposed dynamic scheme.

VI. IEEE 9-BUS DISTRIBUTION NETWORK MODEL

A. DESCRIPTION OF THE PROPOSED POWER NETWORK

The SPOC and HPOC are tested using an IEEE 9-bus test system. The IEEE 9-bus (two feeders) test system is representing the Canadian Urban Benchmark 4-bus feeder system, as shown in Fig. 5. This proposed power network as benchmark network is fed by the main utility supply

has a 500 MVA short-circuit capabilities, 6 X/R ratio, and 500 meter cable length through 20 MVA, 115/12.47 kV sub-transformer with 10% leakage reactance. The system is connected through bus bars B5 and B7 with two PV generation systems thorough 4 MVA transformers (Delta-Y with ground). The detailed information for the power system and PV are described in [7], [26], and [27]. The power network described in Fig. 5 contains 9 non-directional OCRs (R1 to R9) and 6 Directional OCRs (R10 to R15). The initial Current Transformer Ratio (CTR) and Pickup Current for Phase (IP) and Pickup Current for the earth (IPZ) of each OCR adapted through load flow and short circuit calculations according to IEC-60909 are shown in Table 2 [3], [4], [5], [6], [7], [8], [9], [10]. Consequently, the system impedance and admittance required for short-circuit calculations in this study using the ETAP package are attained through the data presented in Table 3 for two operation modes (with and without DG).

The ratio of zero impedance to positive impedance, Z_0/Z_1 , when three-phase faults occur, is presented in Table 3 under the two operating modes for the network:

- Mode 1 (load only): the proposed power network is fed only by the utility source.
- Mode 2 (with PV): the network is integrated with two PV-generation systems, as previously described.

It can be observed from Table 3 that the Z_0/Z_1 ratio is significantly changed in the two modes in case of fault as a result of the change in the configuration of DG-Interconnection transformers. For example, the Z_0/Z_1 ratio was 3.19 and 1.11 at F1 for Mode 1 and 2, respectively. Therefore, it may be challenging for distribution network

TABLE 6. The short-circuit analysis and TMS setting for OCR based on SPOC and HPOC approaches (Mode 1, Scenario 2 and 3).

Location of fault	Relays	SPOC				HPOC				LLG				IPV			
		LG R=10	IPV	SPOC	HPOC	LG R=30	IPV	SPOC	HPOC	LLG R=10	IPV	SPOC	HPOC	LLG R=30	IPV	SPOC	HPOC
F1	OC1	696	194	0.52	0.13	254	10.30	No Trip	0.105	363	194	No Trip	0.12	128	10	No Trip	0.13
	OC2	696	194	1.71	0.445	254	10.30	No Trip	0.342	363	194	No Trip	0.39	128	10	No Trip	0.43
F2	OC2	714	201	1.65	0.44	256	10.52	No Trip	0.344	369	201	No Trip	0.39	129	10	No Trip	0.42
	OC3	714	201	2.8	0.76	256	10.52	No Trip	0.592	369	201	No Trip	0.67	129	10	No Trip	0.73
F3	OC3	731	205	2.71	0.75	258	10.75	No Trip	0.595	375	205	No Trip	0.66	130	10	No Trip	0.73
	OC4	731	205	3.89	1.08	258	10.75	No Trip	0.859	375	205	No Trip	0.94	130	10	No Trip	1.0
F4	OC4	749	212	3.76	1.07	260	10.97	No Trip	0.863	382	212	No Trip	0.93	131	10	No Trip	1.0
	OC5	749	212	4.96	1.41	260	10.97	No Trip	1.148	382	212	No Trip	1.23	131	10	No Trip	1.38
F5	OC6	696	194	0.52	0.52	254	10.30	No Trip	0.105	363	194	No Trip	0.12	128	10	No Trip	0.13
	OC7	696	194	1.71	1.71	254	10.30	No Trip	0.342	363	194	No Trip	0.39	128	10	No Trip	0.43
F6	OC7	714	201	1.65	1.65	256	10.52	No Trip	0.344	369	201	No Trip	0.39	129	10	No Trip	0.42
	OC8	714	201	2.8	2.8	256	10.52	No Trip	0.592	369	201	No Trip	0.67	129	10	No Trip	0.73
F7	OC8	731	205	2.71	2.71	258	10.75	No Trip	0.595	375	205	No Trip	0.66	130	10	No Trip	0.73
	OC9	731	205	3.89	3.89	258	10.75	No Trip	0.859	375	205	No Trip	0.94	130	10	No Trip	1.05
F8	OC9	749	212	3.76	3.76	260	10.97	No Trip	0.863	382	212	No Trip	0.93	131	10	No Trip	1.05
	OC5	749	212	4.96	4.96	260	10.97	No Trip	1.148	382	212	No Trip	1.23	131	10	No Trip	1.38

operators to reach detailed and determinate settings for earth fault relays, especially in the cases of active distribution networks, as described in Section 3. Furthermore, the initial Time Multiplying Setting (TMS) for each OCR in the network is presented in Table 4 under the two operational modes for the power network.

B. POWER NETWORK - MODE 1 TEST RESULTS

In this section, LG and LLG faults are generated at the proposed power network, as described in Fig. 5 and Table 3 within three different resistance fault scenarios. The fault resistances (R) are conceded to be equal to as 0, 10 and 30 Ohm which represents Scenarios 1 to 3, respectively. Firstly, the R=0 ohm is considered to evaluate the SPOC and HPOC under the first sub-dynamic scheme (area A), where the HPOC will improve the reliability of the

protection system by virtually increasing the fault current component, as described in Section 3. Table 5 shows the zero-sequence current, i_0 , and the virtual fault current (IFV) and the TMS value. As expected, the faults had high short-circuited capabilities due to the diminutive value of the ground resistance.

The proposed HPOC will detect and trip the faults quickly compared to the SPOC to the large magnification of the fault current (IFV) compared to the actual fault current. In the HPOC, the IFV value for both LG and LLG faults became very high, seen by OCRs in the network, and thus the OCRs trip the faults concisely. For example, the actual LG fault current was 3585 A and the IFV was 57539 A at F3. In addition, Fig. 6 and Fig. 7 show time characteristics curves for the SPOC and HPOC for LG fault at F6 and LLG fault at F4, respectively. In Fig. 6, the fault value becomes 44472 A for

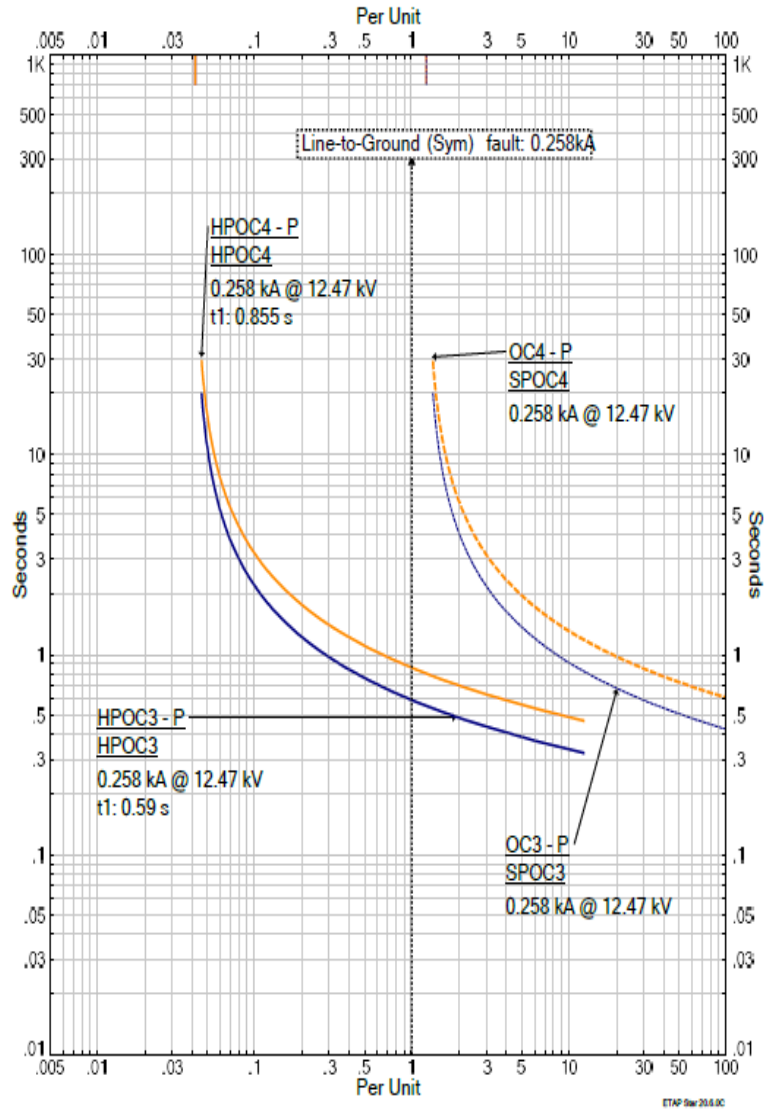


FIGURE 8. Time current characteristics of OC3 and OC4 at scenario 3 (R=30 ohm) for Mode 1 and LG fault.

OC8 and OC7 as IFV which will be used by HPOC compared to the actual fault current (3144 A) which will be used by the SPOC approach. This helped the HPOC achieve the minimum tripping time of 0.395 seconds compared to 0.86 second for SPOC in the OC8. These results showed that the HPOC improved the speed of time tripping by 54% compared to SPOC. The LLG fault at F4 between OC4 and OC5 is shown in Fig. 5. The IFV value was 42885 A compared to 1032 A for the actual fault current, which provides a short tripping time of 0.55 seconds for OC4 by HPOC compared to 1.26 seconds by SPOC, as shown in Fig. 7. This fast and properly tripping time will offer a selective and reliable performance for the OCR scheme in the network and enhance its stability.

Now, the R=10 and 30 ohm (scenarios 1 and 2) are applied to investigate the performance of SPOC and HPOC approaches under the second sub-dynamic scheme (area B),

where the HPOC will work on covering all the possible phase and earth faults and minimize the tripping time by adapting the pickup current as virtual pickup current (IPV), as described in Section 3. Table 6 shows the zero-sequence current, i_0 , and the virtual pickup current (IPV) and the TMS value for LG and LLG faults. LG and LLG faults in Scenarios 1 and 2 had low short-circuited capabilities compared to solid faults due to ground resistance. Therefore, the OCRs will normally take long time to trip the fault or will be not able to discover it, as discussed in Section 3. The proposed HPOC will detect and trip the faults quickly compared to the SPOC by adapting the pickup current (IPV).

Fig. 8 shows the time current characteristics of OC3 and OC4 at scenario 3 (R=30 ohm) and LG fault (F3) for the SPOC and HPOC. The LG fault (F3) will be seen by both OCRs (OC3 and OC4) with a IPV of 10.75 by employing the

TABLE 7. The short-circuit analysis and TMS setting for OCRs based on SPOC and HPOC approaches (Mode 2, LG, Scenario 1 to 3).

Location of fault	Relays	LG R=0	IFV	IPV	SPOC	HPOC	LG R=10	IPV	SPOC	HPOC	LG R=30	IPV	SPOC	HPOC
F1	OC1	3682	55792.53		0.147	0.065	459	35.1	1.43	0.132	140	3.2	NO TRIP	0.089
	OC2	3682	55792.53		0.476	0.213	459	35.1	4.65	0.429	140	3.2	NO TRIP	0.288
	OC12	1066	6297.296		0.387	0.163	287	17.9	NO TRIP	0.202	180	7.2	NO TRIP	0.157
F2	OC2	4075	74821.53		0.456	0.201	484	37.6	3.82	0.480	136	2.8	NO TRIP	0.280
	OC3	4075	74821.53		0.785	0.346	484	37.6	6.57	0.744	136	2.8	NO TRIP	0.483
	OC13	968	4943.714		0.373	0.158	265	15.7	NO TRIP	0.177	173	6.5	NO TRIP	0.138
	OC12	968	4943.714		0.418	0.177	265	15.7	NO TRIP	0.198	173	6.5	NO TRIP	0.154
F3	OC3	4618	96400.75		0.746	0.33	532	42.4	4.98	0.752	132	2.4	NO TRIP	0.468
	OC4	4618	96400.75		1.07	0.47	532	42.4	7.19	1.087	132	2.4	NO TRIP	0.676
	OC13	874		25.5	0.303	0.095	252	14.4	NO TRIP	0.130	166	5.8	NO TRIP	0.100
	OC14	874		25.5	0.35	0.11	252	14.4	NO TRIP	0.151	166	5.8	NO TRIP	0.117
F4	OC4	5387	145074.9		1.01	0.442	544	43.6	6.80	1.089	129	2.1	NO TRIP	0.657
	OC5	5387	145074.9		1.341	0.588	544	43.6	9.05	1.449	255	14.7	NO TRIP	1.277
	OC15	781		22.4	0.33	0.094	212	10.4	NO TRIP	0.123	159	5.1	NO TRIP	0.098
	OC14	781		22.4	0.39	0.109	212	10.4	NO TRIP	0.142	159	5.1	NO TRIP	0.114
F5	OC6	3927	69431		0.143	0.063	724	61.6	0.497	0.138	255	14.7	NO TRIP	0.119
	OC7	3927	69431		0.489	0.215	724	61.6	1.70	0.47	255	14.7	NO TRIP	0.407
F6	OC7	4677	98931		0.454	0.201	741	63.3	1.64	0.47	257	14.9	NO TRIP	0.408
	OC8	3763	63187		0.853	0.376	475	36.7	7.37	0.780	137	2.9	NO TRIP	0.5117 53
F7	OC8	4615	96274		0.783	0.346	489	38.1	6.67	0.783	137	2.9	NO TRIP	0.511
	OC9	4615	96274		1.109	0.491	489	38.1	9.456	1.10	137	2.9	NO TRIP	0.724
F8	OC9	5308	127760		1.05	0.466	532	42.4	7.4	1.11	132	2.4	NO TRIP	0.696
	OC5	4815	104926		1.40	0.62	371	26.3	124	1.38	257	14.9	NO TRIP	1.280
	OC10	979	5069		0.276	0.128	233	12.5	NO TRIP	0.12	155	4.7	NO TRIP	0.096
	OC11	979	5069		0.320	0.149	233	12.5	NO TRIP	0.147	155	4.7	NO TRIP	0.112

HPOC characteristics instead of 258 for HPOC. This makes the tripping time of OC3 become 0.595 seconds by HPOC compared to no trip signal status for SPOC.

C. POWER NETWORK - MODE 2 TEST RESULTS

In this section, the impact of adding DGs to the grid on the performance of SPOC and HPOC is investigated. The LG and LLG faults are generated with fault resistances (R) equal to 0, 10 and 30 Ohm which represents scenarios 1, 2 and 3, respectively. The changing of Z_0/Z_1 ratio due to the availability of DGs in the network increase the complexity of achieving optimal OCR setting, as described in Section 3. The PV generation units in Mode 2 change the behavior and fault characteristics. For example, the LG fault level at F3 and F4 for R=0 ohm was under 900 A, which is very difficult to be detect by SPOC approach and require adapting in the pickup current values. In scenario 2 (R= 10 ohm), the SPOC approach was not able to detect or trip the fault for most of the cases. In addition, the SPOC approach does not work for all fault at scenario 3, where the fault level is low. Therefore, the

significance and feasibility of the HPOC is highly noticeable when the LG faults occurs through earth resistance of 10 and 30 Ohm, as in Tables 7.

The HPOC has use the proposed two sub-dynamic schemes (area A and area B) to improve the reliability of the protection system by virtually increasing the fault current and pickup current components based on their values, as shown in Table 7 (F3 and F4). In addition, the proposed HOPC outperformed the SPOC in term of the minimum time tripping. Fig. 9 shows time characteristics curves for the SPOC and HPOC for LG fault at F2. The HPOC achieve the minimum tripping time at 0.201, 0.346, 0.158 and 0.177 second for OC2, OC3, OC12 and OC14, respectively, compared to 0.456, 0.785, 0.373 and 0.418 second for SPOC. These results showed that the HPOC improved the speed of the total time tripping at F2 by 56.6% compared to SPOC. The LLG fault at F4 between OC4 and OC5 is shown in Fig. 5. The IFV value was 42885 A compared to 1032 A for the actual fault current, which provides a short tripping time of 0.55 second for OC4 by HPOC compared to 1.26 second by SPOC. This fast and properly

TABLE 8. The short-circuit analysis and TMS setting for OCRs based on SPOC and HPOC approaches (Mode 2, LLG, Scenario 1 to 3).

Location of fault	Relays	LLG R=0	IFV	SPOC	HPOC	LLG R=10	IPV	SPOC	HPOC	LLG R=30	IPV	SPOC	HPOC
F1	OC1	4229	80683.84	0.138	0.061	165	5.7	NO TRIP	0.132	56	15	NO TRIP	0.199
	OC2	4229	80683.84	0.449	0.198	165	5.7	NO TRIP	0.429	56	1.1	NO TRIP	0.646
	OC12	1199	7786.363	0.355	0.165	247	13.9	NO TRIP	0.202	84	3.0333	NO TRIP	0.241
F2	OC2	4807	134452.9	0.426	0.180	198	9	NO TRIP	0.480	67	1.711	NO TRIP	0.584
	OC3	4807	104574.5	0.734	0.325	198	9	NO TRIP	0.744	67	2.2	NO TRIP	1.007
	OC13	1038	5746.071	0.353	0.1646	207	9.9	NO TRIP	0.177	70	1.944	NO TRIP	0.236
	OC12	1038	5746.071	0.395	0.184	207	9.9	NO TRIP	0.198	70	1.944	NO TRIP	0.264
F3	OC3	5458	135186.6	0.698	0.310	233	12.5	NO TRIP	0.752	79	3.4	NO TRIP	0.925
	OC4	5458	135186.6	1.009	0.4482	233	12.5	NO TRIP	1.087	79	3.4	NO TRIP	1.336
	OC13	908	4323.81	0.294	0.137	169	6.1	NO TRIP	0.130	57	0.933	NO TRIP	0.197
	OC14	908	4323.81	0.341	0.159	169	6.1	NO TRIP	0.151	57	0.933	NO TRIP	0.229
F4	OC4	6260	178294.1	0.959	0.427	270	16.2	NO TRIP	1.089	91	4.6	NO TRIP	1.249
	OC5	5774	151460.6	1.314	0.584	159	5.1	NO TRIP	1.449	54	0.9	NO TRIP	2.187
	OC15	799	3286.363	0.3303	0.154	133	2.5	NO TRIP	0.123	45	3	NO TRIP	0.229
	OC14	799	3286.363	0.383	0.179	133	2.5	NO TRIP	0.142	45	3	NO TRIP	0.265
F5	OC6	4577	94697.28	0.134	0.059	388	28	NO TRIP	0.138	134	8.9	NO TRIP	0.131
	OC7	4577	94697.28	0.458	0.203	388	28	NO TRIP	0.47	134	8.9	NO TRIP	0.449
F6	OC7	5179	121586.6	0.437	0.1938	396	28.8	NO TRIP	0.47	135	9	NO TRIP	0.448
	OC8	4759	102472.7	0.774	0.342	191	8.3	NO TRIP	0.780	65	2	NO TRIP	1.075
F7	OC8	5359	130278.3	0.739	0.328	195	8.7	NO TRIP	0.783	66	2.1	NO TRIP	1.066
	OC9	5359	130278.3	1.046	0.464	195	8.7	NO TRIP	1.10	66	2.1	NO TRIP	1.510
F8	OC9	6201	174919.9	0.991	0.441	235	12.7	NO TRIP	1.11	79	3.4	NO TRIP	1.376
	OC5	5752	150297.6	1.316	0.585	152	4.4	NO TRIP	1.38	52	0.7	NO TRIP	2.2386
	OC10	1044	5816.571	0.262	0.122	170	6.2	NO TRIP	0.12	57	0.933	NO TRIP	0.197
	OC11	1044	5816.571	0.304	0.1418	170	6.2	NO TRIP	0.147	57	0.933	NO TRIP	0.229

tripping time will offer a selective and reliable performance for the OCR scheme in the network and enhance its stability.

Fig. 10 shows the time current characteristics of relays at F7 (LG) between Bus 6 and Bus 7. The actual value of fault was 137 A due to the high ground resistance of 30 Ohm. This OC8 and OC9 was not able not detect the fault by the SPOC. While the HPOC helped OCR characteristics to detect the fault and disconnect it within minimum time by adjusting the pickup current value to a smaller value than when SPOC characteristics. This providing the possibility for HPOC to isolate the fault F7 in 0.511 and 0.724 second for OC8 and OC9, respectively. This will enhance the OCR scheme performance against high impedance faulty situations created due to the nature of nowadays active distribution networks.

The performance of SPOC and HPOC is also investigated under LLG fault for Mode 2. The LLG faults are generated

with different fault resistances (R) equal to 0, 10 and 30 Ohm. The PV generation units in Mode 2 change the behavior and fault characteristics compare to Mode 1. Table 8 shows that the LLG fault with resistance 10 and 30 ohms is very difficult to be detect by SPOC approach. In scenario 2 and, the SPOC approach was not able to detect or trip the LLG fault for all cases. The high-impedance ground faulty cases will cause network stability issues and reduce the performance of ground fault protection schemes in active, complex, and multi-loop network arrangements. This is showed the significance of the HPOC to detect the fault and isolate within minimum time, as shown in Table 8. In scenario 1 (R= 0 ohm), the HPOC outperformed the SPOC approach in term of detecting and tripping the fault for all of the cases. For example, the HPOC achieve the minimum tripping time at 0.061, 0.198 and 0.165 second for OC1, OC2 and OC12, respectively, compared to 0.138, 0.449 and 0.55 second for

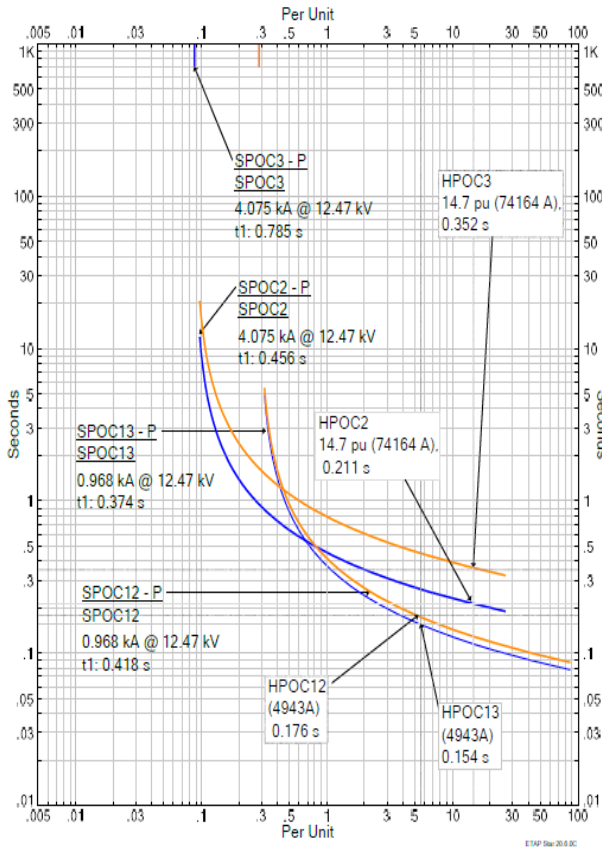


FIGURE 9. Time current characteristics of OC2, OC3, OC12 and OC14 at scenario 1 (R=0 ohm) for Mode 2 and LG fault (F2).

TABLE 9. The OCRs to simulate the IEEE 33-bus network model.

Relay	CTR	IP	IPZ
OC1	200/1	50	10
OC2	200/1	50	10
OC3 to OC32	100/1	50	10

SPOC. These results showed that the HPOC improved the speed of the total time tripping at F1 by 55% compared to SPOC.

D. DISCUSSION AND COMPARISON

The performance of the proposed HPOC and SPOC approaches over two power network modes and three fault sceneries are compared in term of the total tripping time for OCRs (OOT) in this section. Firstly, the OTT for all OCRs in Mode 1 of the power network (without DGs) over LG and LLG faults under three fault scenarios (R=0,10 and 30 ohm) are shown in Fig. 11. The HPOC approach reduced the OTT at LG and LLG faults under scenario 1 and 2 for LG and scenario 1 for LG compared to the SPOC approach. For example, the OTT was 12.17 and 44 second in scenario 2 (LG fault) for HPOC and SPOC approaches, respectively. Fig.11 presented the powerful of the HPOC approach in detecting

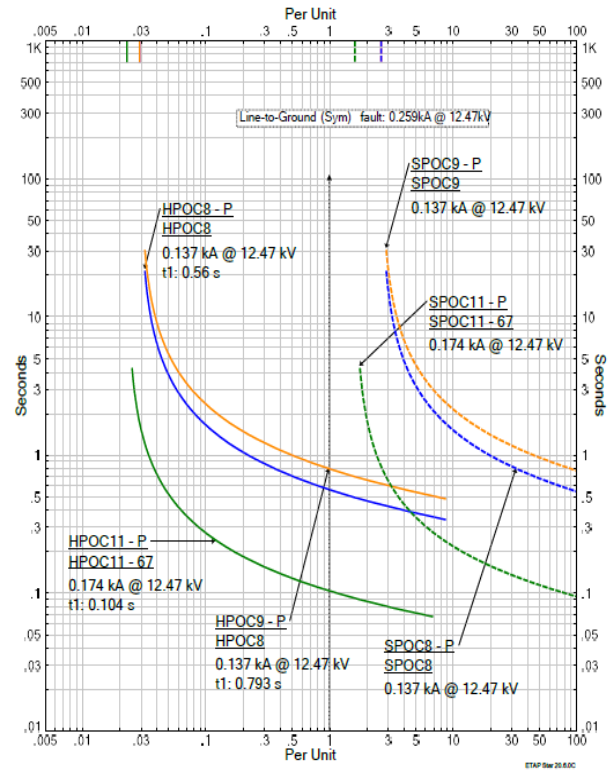


FIGURE 10. Time current characteristics of OC8 and OC9 at scenario 1 (R=30 ohm) for Mode 2 and LG fault (F7).

the low fault current in scenario 3 at LG fault and scenario 2 and 3 at LLG fault compare to SPOC which was not able to detect the faults.

In addition, the HPOC and SPOC approaches are used to handle the changes of adding DGs to the network (Mode 2), as presented in Section 3. The comparison of the HPOC and SPOC for Mode 2 under different fault scenarios are shown in Fig.12. The HPOC outperformed the SPOC in term of minimizing the tripping time (OOT) and detecting the faults. Fig.12 introduced the superiority of the HPOC compared to SPOC in detecting the faults when the fault resistance is high, for example, in scenario 3 at LG fault and scenario 2 and 3 at LLG fault. Furthermore, the HPOC improved the OCRs performance in term of achieve the minimum OOT, for example, the OTT was 13.78 and 203 second in scenario 2 (LG fault) for HPOC and SPOC approaches, respectively.

VII. IEEE 33-BUS DISTRIBUTION NETWORK MODEL

This section aims to use a larger distribution network model (IEEE 33-bus) to evaluate and compare the proposed HPOC and traditional SPOC schemes. Furthermore, the results of this section aim to show the transferability the proposed HPOC scheme to other distribution network. Fig. 13 shows the IEEE-33 bus system, where the maximum and minimum voltage for each bus are limits to range between 10% of its nominal voltage. The IEEE 33-bus is fed through the utility

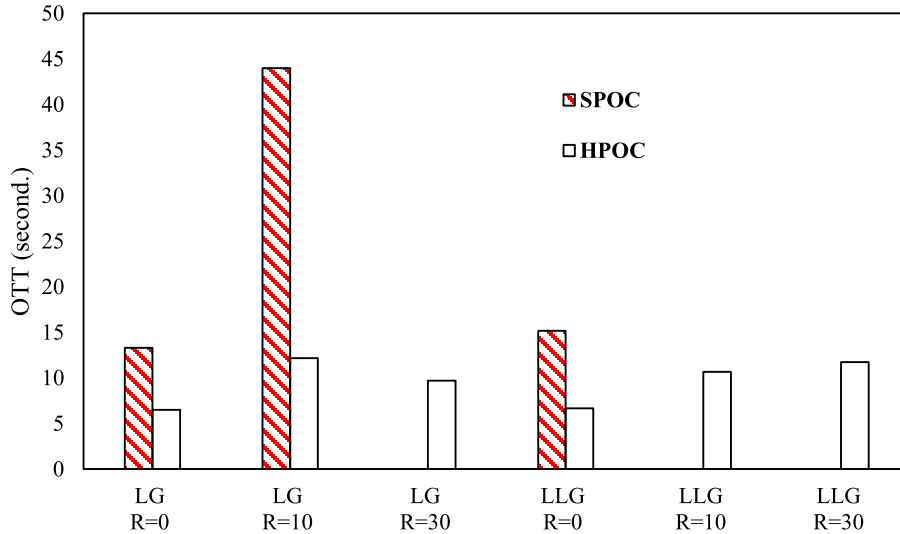


FIGURE 11. The results of SPOC and HPOC approaches over different fault scenario for Mode 1.

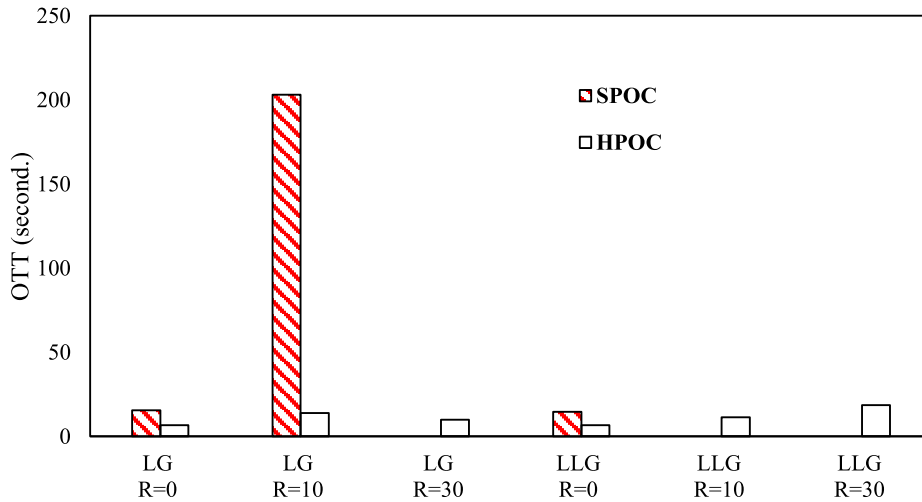


FIGURE 12. The results of SPOC and HPOC approaches over different fault scenario for Mode 2.

TABLE 10. The TMS setting for OCRs at the IEEE 33-bus network model.

Relay	TMS	Relay	TMS
OC1	0.96	OC17	0.01
OC2	0.9	OC18	0.21
OC3	0.84	OC19	0.14
OC4	0.78	OC20	0.07
OC5	0.7	OC21	0.01
OC6	0.67	OC22	0.14
OC7	0.6	OC23	0.07
OC8	0.57	OC24	0.01
OC9	0.5	OC25	0.45
OC10	0.43	OC26	0.38
OC11	0.36	OC27	0.33
OC12	0.3	OC28	0.26
OC13	0.24	OC29	0.19
OC14	0.18	OC30	0.12
OC15	0.12	OC31	0.06
OC16	0.06	OC32	0.01

supply system and the two 4-MW solar power plants. The line data and load information of the simulated system by ETAP is available in [28] and [29]. The IEEE 33-bus system in

Fig. 13 including 32 OCRs and Table 9 presents the PS, CTR and IPZ for each OCR. Furthermore, the initial TMS for each OCR in the IEEE 33-bus system is shown in Table 10. In this

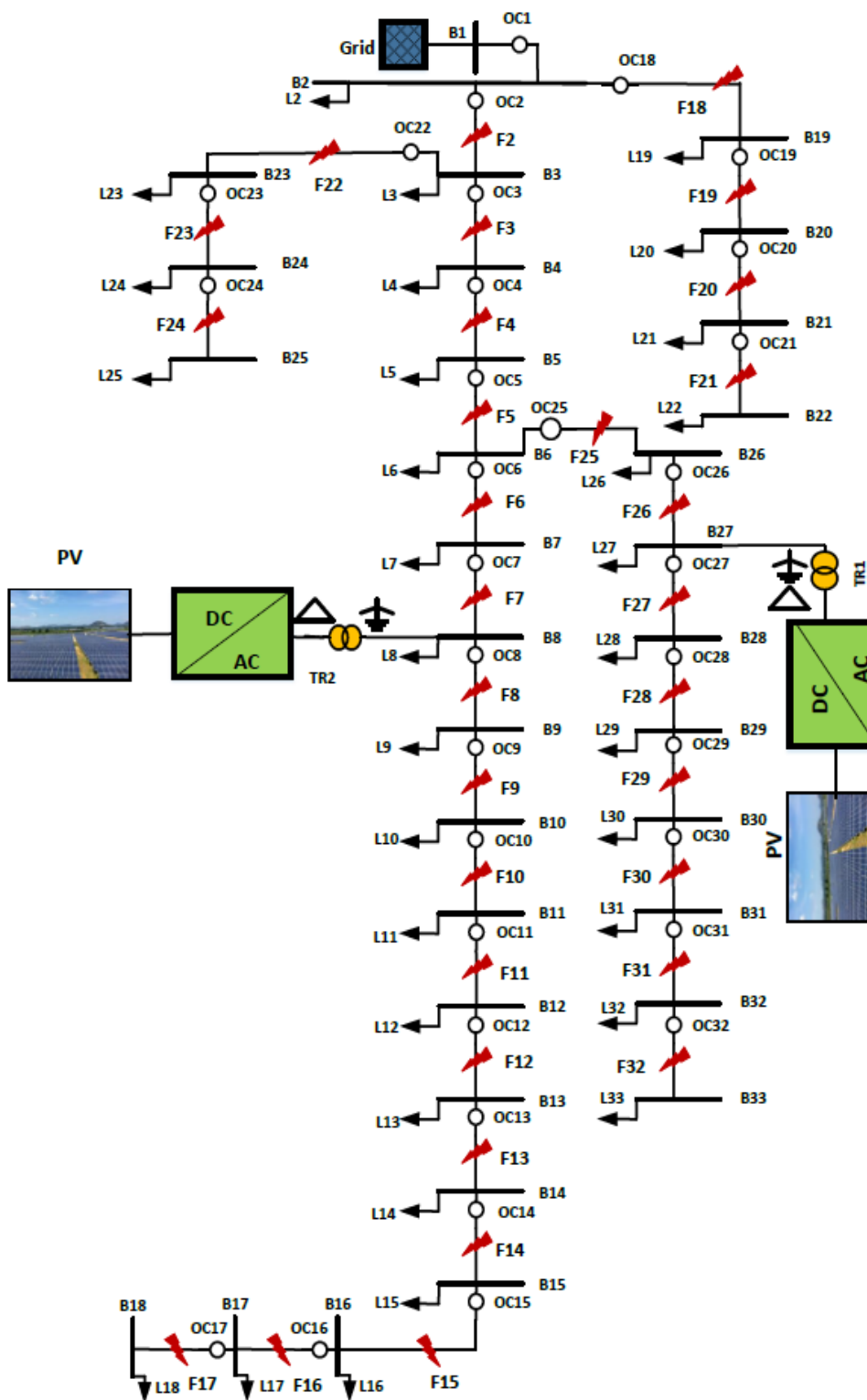


FIGURE 13. IEEE 33-bus microgrid system (large Scale distribution network).

section, LG and LLG faults under different location scenarios are generated at the IEEE 33-bus network, as described in

Fig. 13. The impact of the fault resistances (R) is investigated by employing two fault resistances ($R = 0$ and $R = 30$ Ohm)

TABLE 11. The short-circuit analysis and TMS setting for OCRs based on SPOC and HPOC approaches (IEEE 33-bus, LLG under R=0 ohm, LG under R=30 ohm).

Location of fault	Relays	LLG R=0	IFV	SPOC	HPOC	Location of fault	Relays	LG R=30	IFV	SPOC	HPOC
LLG						LG					
F2	OC2	252.8	84.3	3.8	1.7	F18	OC18	245.9	1770.0	0.9	0.4
	OC1	252.8	84.3	4.1	1.8		OC1	79.5	131.2	4.1	1.9
F3	OC3	241.6	80.5	3.7	1.6	F19	OC19	235.9	1618.3	0.6	0.3
	OC2	241.6	80.5	3.9	1.7		OC18	235.9	1618.3	0.9	0.4
F4	OC4	232.8	77.6	3.5	1.5	F20	OC20	225.8	1473.4	0.3	0.1
	OC3	232.8	77.6	3.8	1.6		OC19	225.8	1473.4	0.6	0.3
F5	OC5	208.8	69.6	3.4	1.5	F21	OC21	216.8	1349.5	0.0	0.0
	OC4	208.8	69.6	3.8	1.6		OC20	216.8	1349.5	0.3	0.1
F6	OC6	224.8	74.9	3.1	1.3	F22	OC22	233.2	1579.5	0.6	0.3
	OC5	224.8	74.9	3.2	1.4		OC2	151.6	614.3	3.9	1.7
F7	OC7	248.0	82.7	2.6	1.1	F23	OC23	233.2	1579.5	0.3	0.1
	OC6	132.0	44.0	4.8	2.3		OC22	233.2	1579.5	0.6	0.3
F8	OC8	332.0	110.7	2.1	0.9	F24	OC24	223.7	1443.8	0.0	0.0
	OC7	155.2	51.7	3.7	1.6		OC23	223.7	1443.8	0.3	0.1
F9	OC9	316.0	105.3	1.9	0.8	F25	OC25	183.9	943.5	2.4	1.0
	OC8	316.0	105.3	2.1	0.9		OC5	135.7	478.0	3.7	1.6
F10	OC10	312.0	104.0	1.6	0.7	F26	OC26	224.7	1458.6	1.7	0.8
	OC9	312.0	104.0	1.9	0.8		OC25	224.7	1458.6	2.1	0.9
F11	OC11	309.6	103.2	1.4	0.6	F27	OC27	224.2	1451.2	1.5	0.7
	OC10	309.6	103.2	1.6	0.7		OC26	224.2	1451.2	1.7	0.8
F12	OC12	306.4	102.1	1.1	0.5	F28	OC28	215.7	1335.3	1.2	0.5
	OC11	306.4	102.1	1.4	0.6		OC27	215.7	1335.3	1.6	0.7
F13	OC13	284.0	94.7	1.0	0.4	F29	OC29	207.8	1231.0	0.9	0.4
	OC12	284.0	94.7	1.2	0.5		OC28	207.8	1231.0	1.3	0.6
F14	OC14	274.4	91.5	0.7	0.3	F30	OC30	200.3	1137.5	0.6	0.3
	OC13	274.4	91.5	1.0	0.4		OC29	200.3	1137.5	0.9	0.4
F15	OC15	267.2	89.1	0.5	0.2	F31	OC31	192.9	1047.7	0.3	0.1
	OC14	267.2	89.1	0.7	0.3		OC30	192.9	1047.7	0.6	0.3
F16	OC16	258.4	86.1	0.3	0.1	F32	OC32	187.1	979.7	0.1	0.0
	OC15	258.4	86.1	0.5	0.2		OC31	187.1	979.7	0.3	0.1
F17	OC17	240.0	80.0	0.0	0.0						
	OC16	240.0	80.0	0.3	0.1						

to tackle the two sub-dynamic schemes (area A and area B), as discussed in previous section.

The results shows that the HPOC handle the challenges of OCRs and EF coordination in IEEE 33-bus system similarly to his performance at IEEE 9-bus system. The short-circuit analysis and TMS setting for OCRs based on SPOC and HPOC approaches for IEEE 33-bus with two PV plants for LLG fault with R= 0 ohm and LG fault with R= 30 ohm are presented in Table 11 as a comparison example. The proposed

HOPC detected the faults quickly compared to the SPOC by having the large magnification of the fault current (IFV) compared to actual fault current. In Table 11, the actual LG fault current was 235 A and the IFV was 16818 A at F19, which helped the HPOC achieve the minimum tripping time (OOT). Table 12 shows that the HPOC approach reduced the OTT at LG and LLG faults under fault scenarios (R=0 and R=30) compared to the SPOC approach. The OTT was 81.8 and 129.4 second at LG fault with R = 0 and 10 ohms for SPOC

TABLE 12. The total tripping time (OOT) results of SPOC and HPOC approaches over different fault scenario for IEEE 33-bus.

	LG R=0	LG R=30	LLG R=0	LLG R=30
SPOC	81.8	129.4	93.8	181.56
HPOC	36.06	57.6	41.3	95.31

approach, respectively, compared to 36.06 and 57.6 seconds for HPOC approach, respectively. In addition, the HPOC approach achieved an OTT reduction by 56% and 47.5% compared to SPOC for LLG with R=0 and R=30 ohms, respectively.

VIII. CONCLUSION AND RECOMMENDATIONS

In this article, a novel dynamic and hybrid OCR scheme has been presented for solving the protection coordination problem in power network equipped with or without PV generations. In the HPOC, the setting of all OCRs is adjusted and adapted by using two sub-schemes which modifying the fault and pickup currents (IFV and IPV). The proposed HPOC approach minimizes the tripping time (OTT) for all OCRs under different fault location and characteristic by 60% and 55.5% compared to SPOC for LG with R=0 at IEEE 9-bus and 33-bus systems, respectively. The outcomes of the HPOC approach in all operational network modes and fault scenarios (fault types: LG and LLG, and impedances), the OOT was notably decreased compared to SPOC. In addition, the HPOC approach showed powerful performance in detecting the low fault current in scenario 2 and 3 at LG and LLG faults compare to SPOC which was not able to detect these faults. Furthermore, the PSO algorithm was employed to solve the optimization problem and achieve the minimum OTT for the HPOC and SPOC approaches. Finally, the miss-coordination problem for EF and OC relays is eliminated in this work by using the new HPOC approach. In the future, the proposed HPOC approach will be adapted for distance relays protection model.

REFERENCES

- [1] N. Cho, M. Yoon, and S. Choi, "Impact of transformer topology on short-circuit analysis in distribution systems with inverter-based distributed generations," *Sustainability*, vol. 14, no. 15, p. 9781, Aug. 2022, doi: 10.3390/su14159781.
- [2] J. Mohammadi, F. B. Ajaei, and G. Stevens, "Grounding the AC microgrid," *IEEE Trans. Ind. Appl.*, vol. 55, no. 1, pp. 98–105, Jan. 2019.
- [3] Q. Jia, X. Dong, and S. Mirsaedi, "A traveling-wave-based line protection strategy against single-line-to-ground faults in active distribution networks," *Int. J. Electr. Power Energy Syst.*, vol. 107, pp. 403–411, May 2019.
- [4] B. Polajžer, M. Pintarič, J. Ribič, M. Rošer, and G. Štumberger, "Parametrization of ground-fault relays in MV distribution networks with resonant grounding," *Int. J. Electr. Power Energy Syst.*, vol. 143, Dec. 2022, Art. no. 108449.
- [5] A. B. Nassif, E. Loi, K. A. Wheeler, and S. Bahramirad, "Impact of IBR negative-sequence current injection on ground fault temporary overvoltage and ground overcurrent protection," in *Proc. IEEE/PES Transmiss. Distrib. Conf. Expo. (TD)*, Apr. 2022, pp. 25–28, doi: 10.1109/TD43745.2022.9816974.
- [6] J. Andruszkiewicz, J. Lorenc, B. Staszak, A. Weychan, and B. Zięba, "Overcurrent protection against multi-phase faults in MV networks based on negative and zero sequence criteria," *Int. J. Electr. Power Energy Syst.*, vol. 134, Jan. 2022, Art. no. 107449.
- [7] N. El-Naily, S. M. Saad, A. Elhaffar, E. Zarour, and F. Alasali, "Innovative adaptive protection approach to maximize the security and performance of phase/earth overcurrent relay for microgrid considering earth fault scenarios," *Electr. Power Syst. Res.*, vol. 206, May 2022, Art. no. 107844.
- [8] P. T. Manditereza and R. Bansal, "Renewable distributed generation: The hidden challenges—A review from the protection perspective," *Renew. Sustain. Energy Rev.*, vol. 58, pp. 1457–1465, May 2016.
- [9] V. Telukunta, J. Pradhan, A. Agrawal, M. Singh, and S. G. Srivani, "Protection challenges under bulk penetration of renewable energy resources in power systems: A review," *CSEE J. Power Energy Syst.*, vol. 3, no. 4, pp. 365–379, Dec. 2017.
- [10] M. Chabanlooa, G. Malekia, M. Agah, and M. Habashic, "Comprehensive coordination of radial distribution network protection in the presence of synchronous distributed generation using fault current limiter," *Int. J. Electr. Power Energy Syst.*, vol. 99, pp. 214–224, Jul. 2018.
- [11] A. B. Nassif and A. Electric, "A protection and grounding strategy for integrating inverter-based distributed energy resources in an isolated microgrid," *CPSS Trans. Power Electron. Appl.*, vol. 5, no. 3, pp. 242–250, Sep. 2020.
- [12] A. H. A. Bakar, H. Mokhlis, H. A. Illias, and P. L. Chong, "The study of directional overcurrent relay and directional earth-fault protection application for 33kV underground cable system in Malaysia," *Int. J. Electr. Power Energy Syst.*, vol. 40, no. 1, pp. 113–119, Sep. 2012.
- [13] K. A. Saleh, H. H. Zeineldin, A. Al-Hinai, and E. F. El-Saadany, "Optimal coordination of directional overcurrent relays using a new time-current-voltage characteristic," *IEEE Trans. Power Del.*, vol. 30, no. 2, pp. 537–544, Apr. 2015, doi: 10.1109/TPWRD.2014.2341666.
- [14] H. Muda and P. Jena, "Superimposed adaptive sequence current based microgrid protection: A new technique," *IEEE Trans. Power Del.*, vol. 32, no. 2, pp. 757–767, Apr. 2017.
- [15] A. Sharma and B. K. Panigrahi, "Phase fault protection scheme for reliable operation of microgrids," *IEEE Trans. Ind. Appl.*, vol. 54, no. 3, pp. 2646–2655, May 2018.
- [16] H. Muda and P. Jena, "Sequence currents based adaptive protection approach for DNs with distributed energy resources," *IET Gener., Transmiss. Distrib.*, vol. 11, no. 1, pp. 154–165, Jan. 2017.
- [17] E. Purwar, S. P. Singh, and D. N. Vishwakarma, "A robust protection scheme based on hybrid pick-up and optimal hierarchy selection of relays in the variable DGs-distribution system," *IEEE Trans. Power Del.*, vol. 35, no. 1, pp. 150–159, Feb. 2020.
- [18] P. Mishra, A. K. Pradhan, and P. Bajpai, "Positive sequence relaying method for solar photovoltaic integrated distribution system," *IEEE Trans. Power Del.*, vol. 36, no. 6, pp. 3519–3528, Dec. 2021.
- [19] M. F. Shaikh, S. Katyara, Z. H. Khand, M. A. Shah, L. Staszewski, V. Bhan, A. Majeed, S. Shaikh, and L. Zbigniew, "Novel protection coordination scheme for active distribution networks," *Electronics*, vol. 10, no. 18, p. 2312, Sep. 2021, doi: 10.3390/electronics10182312.
- [20] E. Sorrentino and J. V. Rodríguez, "Effects of fault type and pre-fault load flow on optimal coordination of directional overcurrent protections," *Electr. Power Syst. Res.*, vol. 213, Dec. 2022, Art. no. 108685.
- [21] P. Naveen and P. Jena, "A robust protection scheme for multimicrogrids using fault current limiter," *IEEE Trans. Ind. Appl.*, vol. 58, no. 5, pp. 5763–5775, Sep. 2022.
- [22] A. Conde and M. Y. Shih, "An adaptive overcurrent coordination scheme withstanding active network operations," *IEEE Access*, vol. 10, pp. 104270–104284, 2022, doi: 10.1109/ACCESS.2022.3210538.
- [23] A. Atae-Kachoe, H. Hashemi-Dezaki, and A. Ketabi, "Optimized adaptive protection coordination of microgrids by dual-setting directional overcurrent relays considering different topologies based on limited independent relays' setting groups," *Electr. Power Syst. Res.*, vol. 214, Jan. 2023, Art. no. 108879.
- [24] R. Aazami, S. Esmailbeigi, M. Valizadeh, and M. S. Javadi, "Novel intelligent multi-agents system for hybrid adaptive protection of microgrid," *Sustain. Energy, Grids Netw.*, vol. 30, Jun. 2022, Art. no. 100682.
- [25] A. A. Balyith, H. M. Sharaf, M. Shaaban, E. F. El-Saadany, and H. H. Zeineldin, "Non-communication based time-current-voltage dual setting directional overcurrent protection for radial distribution systems with DG," *IEEE Access*, vol. 8, pp. 190572–190581, 2020, doi: 10.1109/ACCESS.2020.3029818.
- [26] F. Alasali, N. El-Naily, E. Zarour, and S. M. Saad, "Highly sensitive and fast microgrid protection using optimal coordination scheme and nonstandard tripping characteristics," *Int. J. Electr. Power Energy Syst.*, vol. 128, Jun. 2021, Art. no. 106756.

- [27] F. Alasali, E. Zarour, W. Holderbaum, and K. N. Nusair, "Highly fast innovative overcurrent protection scheme for microgrid using Metaheuristic optimization algorithms and nonstandard tripping characteristics," *IEEE Access*, vol. 10, pp. 42208–42231, 2022.
- [28] M. Baran and F. Wu, "Network reconfiguration in distribution systems for loss reduction and load balancing," *IEEE Trans. Power Del.*, vol. PD-4, no. 2, pp. 1401–1407, Apr. 1989.
- [29] V. Vita, "Development of a decision-making algorithm for the optimum size and placement of distributed generation units in distribution networks," *Energies*, vol. 10, p. 1433, Sep. 2017, doi: 10.3390/en10091433.



SAHBAN W. ALNASER (Member, IEEE) received the Ph.D. degree in electrical power systems from The University of Manchester, U.K., in 2015. He was a Postdoctoral Research Associate in network integration of PV and storage at The University of Manchester. From 2005 to 2011, he was with Electricity Distribution Company (EDCO), Jordan, as the Head of Power System Studies. He is currently an Assistant Professor in electrical power systems at the Department of Electrical Engineering, The University of Jordan. His research interests include grid integration of renewable energy sources, demand response, and energy storage systems.



FERAS ALASALI received the Ph.D. degree in electrical power engineering from the University of Reading, in 2019. He is currently an Assistant Professor with the Department of Electrical Engineering, The Hashemite University, Jordan, with more than five years of experience in optimal and predictive control models for energy storage systems and LV network applications, where he is also the Director of the Renewable Energy Center. His research interests include control models for distributed generation, renewable energy sources, energy storage and LV networks, load forecasting, and power protection systems.



WILLIAM HOLDERBAUM (Member, IEEE) has been working at the University of Glasgow, the University of Reading, Manchester Metropolitan University, and Aston University, and currently held the Professor status in control engineering at the University of Salford, U.K. He has played major leadership roles in research, whilst maintaining a very strong international reputation and an extensive list of publications and Ph.D.'s supervisions. Over the years, he has applied his control expertise to several applications and in particular rehabilitation engineering and energy transmission, storage for electrical systems, and power systems.



ABDELAZIZ SALAH SAÏDI (Member, IEEE) was born in Tunisia, in 1979. He received the M.S. degree in electrical systems from the National Engineering School of Tunis, in 2003, and the Ph.D. degree in electrical engineering from the National Engineering School of Tunis, in 2011. He is currently an Associate Professor in electrical engineering at King Khalid University, Abha. His research interests include dynamical systems theory applied to power systems integrating renewable energy, power systems voltage stability using load flow techniques, and power systems control and operation.



SAAD M. SAAD was born in Al-Brega, Libya, in 1985. He received the B.S. degree from the School of Electrical Engineering, Benghazi University, Benghazi, Libya, in 2009, and the M.Sc. degree from Benghazi University, in 2015, both in electrical engineering. He is currently a Lecturer at the College of Electrical and Electronics Technology-Benghazi, Libya. His research interests include the impact of integrating renewable energy sources on protection systems in active distribution networks and microgrids and power quality.



NASER EL-NAÏLY was born in Libya. He received the B.Sc. and M.Sc. degrees from the University of Benghazi, Libya, in 2010. His current research interests include power system protection and control, distributed generation, microgrids, intelligent grids, applications of artificial intelligence, and to the integration of renewable energy and distributed generation into Libyan electric grids.



MAHMOUD GAMALELDIN received the master's degree in renewable energy engineering from Heriot-Watt University. He is currently the Head of the Power System Studies & Protection Unit, Saudi Aramco. His research interests include the impact of integrating renewable energy sources on power and protection systems in distribution networks and power systems voltage stability using load flow techniques.

...